Results from a search for dark matter in the complete LUX exposure

Supplementary Material

D.S. Akerib,[1,2,3] S. Alsum,[4] H.M. Araújo,[5] X. Bai,[6] A.J. Bailey,[5] J. Balajthy,[7] P. Beltrame,[8] E.P. Bernard,[9,10] A. Bernstein,[11] T.P. Biesiadzinski,[1,2,3] E.M. Boulton,[9,10] R. Bramante,[1,2,3] P. Brás,[12] D. Byram,[13,14] S.B. Cahn,[10] M.C. Carmona-Benitez,[15] C. Chan,[16] A.A. Chiller,[13] C. Chiller,[13] A. Currie,[5] J.E. Cutter,[17] T.J.R. Davison,[8] A. Dobi,[18] J.E.Y. Dobson,[19] E. Druszkiewicz,[20] B.N. Edwards,[10] C.H. Faham,[18] S. Fiorucci,[16,18] R.J. Gaitskell,[16] V.M. Gehman,[18] C. Ghag,[19] K.R. Gibson,[1] M.G.D. Gilchriese,[18] C.R. Hall,[7] M. Hanhardt,[6,14] S.J. Haselschwardt,[15] S.A. Hertel,[9,10,*] D.P. Hogan,[9] M. Horn,[14,9,10] D.Q. Huang,[16] C.M. Ignarra,[2,3] M. Ihm,[9] R.G. Jacobsen,[9] W. Ji,[1,2,3] K. Kamdin,[9] K. Kazkaz,[11] D. Khaitan,[20] R. Knoche,[7] N.A. Larsen,[10] C. Lee,[1,2,3] B.G. Lenardo,[17,11] K.T. Lesko,[18] A. Lindote,[12] M.I. Lopes,[12] A. Manalaysay,[17,†] R.L. Mannino,[21] M.F. Marzioni,[8] D.N. McKinsey,[9,18,10] D.-M. Mei,[13] J. Mock,[22] M. Moongweluwan,[20] J.A. Morad,[17] A.St.J. Murphy,[8] C. Nehrkorn,[15] H.N. Nelson,[15] F. Neves,[12] K. O'Sullivan,[9,18,10] K.C. Oliver-Mallory,[9] K.J. Palladino,[4,2,3] E.K. Pease,[9,18,10] P. Phelps,[1] L. Reichhart,[19] C. Rhyne,[16] S. Shaw,[19] T.A. Shutt,[1,2,3] C. Silva,[12] M. Solmaz,[15] V.N. Solovov,[12] P. Sorensen,[18] S. Stephenson,[17] T.J. Sumner,[5] M. Szydagis,[22] D.J. Taylor,[14] W.C. Taylor,[16] B.P. Tennyson,[10] P.A. Terman,[21] D.R. Tiedt,[6] W.H. To,[1,2,3] M. Tripathi,[17] L. Tvrznikova,[9,10] S. Uvarov,[17] J.R. Verbus,[16] R.C. Webb,[21] J.T. White,[21] T.J. Whitis,[1,2,3] M.S. Witherell,[18] F.L.H. Wolfs,[20] J. Xu,[11] K. Yazdani,[5] S.K. Young,[22] and C. Zhang[13]

(LUX Collaboration)

[1]*Case Western Reserve University, Department of Physics, 10900 Euclid Ave, Cleveland, OH 44106, USA*
[2]*SLAC National Accelerator Laboratory, 2575 Sand Hill Road, Menlo Park, CA 94205, USA*
[3]*Kavli Institute for Particle Astrophysics and Cosmology, Stanford University, 452 Lomita Mall, Stanford, CA 94309, USA*
[4]*University of Wisconsin-Madison, Department of Physics, 1150 University Ave., Madison, WI 53706, USA*
[5]*Imperial College London, High Energy Physics, Blackett Laboratory, London SW7 2BZ, United Kingdom*
[6]*South Dakota School of Mines and Technology, 501 East St Joseph St., Rapid City, SD 57701, USA*
[7]*University of Maryland, Department of Physics, College Park, MD 20742, USA*
[8]*SUPA, School of Physics and Astronomy, University of Edinburgh, Edinburgh EH9 3FD, United Kingdom*
[9]*University of California Berkeley, Department of Physics, Berkeley, CA 94720, USA*
[10]*Yale University, Department of Physics, 217 Prospect St., New Haven, CT 06511, USA*
[11]*Lawrence Livermore National Laboratory, 7000 East Ave., Livermore, CA 94551, USA*
[12]*LIP-Coimbra, Department of Physics, University of Coimbra, Rua Larga, 3004-516 Coimbra, Portugal*
[13]*University of South Dakota, Department of Physics, 414E Clark St., Vermillion, SD 57069, USA*
[14]*South Dakota Science and Technology Authority, Sanford Underground Research Facility, Lead, SD 57754, USA*
[15]*University of California Santa Barbara, Department of Physics, Santa Barbara, CA 93106, USA*
[16]*Brown University, Department of Physics, 182 Hope St., Providence, RI 02912, USA*
[17]*University of California Davis, Department of Physics, One Shields Ave., Davis, CA 95616, USA*
[18]*Lawrence Berkeley National Laboratory, 1 Cyclotron Rd., Berkeley, CA 94720, USA*
[19]*Department of Physics and Astronomy, University College London, Gower Street, London WC1E 6BT, United Kingdom*
[20]*University of Rochester, Department of Physics and Astronomy, Rochester, NY 14627, USA*
[21]*Texas A & M University, Department of Physics, College Station, TX 77843, USA*
[22]*University at Albany, State University of New York, Department of Physics, 1400 Washington Ave., Albany, NY 12222, USA*

(Dated: December 2, 2016)

We report constraints on spin-independent weakly interacting massive particle (WIMP)-nucleon scattering using a 3.35×10^4 kg-day exposure of the Large Underground Xenon (LUX) experiment. A dual-phase xenon time projection chamber with 250 kg of active mass is operated at the Sanford Underground Research Facility under Lead, South Dakota (USA). With roughly four-fold improvement in sensitivity for high WIMP masses relative to our previous results, this search yields no evidence of WIMP nuclear recoils. At a WIMP mass of $50\,\mathrm{GeV}\,c^{-2}$, WIMP-nucleon spin-independent cross sections above $2.2\times10^{-46}\,\mathrm{cm}^2$ are excluded at the 90% confidence level. When combined with the previously reported LUX exposure, this exclusion strengthens to $1.1\times10^{-46}\,\mathrm{cm}^2$ at $50\,\mathrm{GeV}\,c^{-2}$.

* hertel@berkeley.edu
† aaronm@ucdavis.edu

The simulated 3-D electric-field maps in WS2014–16 are constructed by comparing the spatial distribution, in observed coordinates, of a physically uniform calibration source ($^{83\mathrm{m}}$Kr) to that predicted by the field model. The observed coordinates measure the electron drift time and the x-y position of electrons as they leave the liquid surface. Figure 1 shows one method of comparing model to data (see caption).

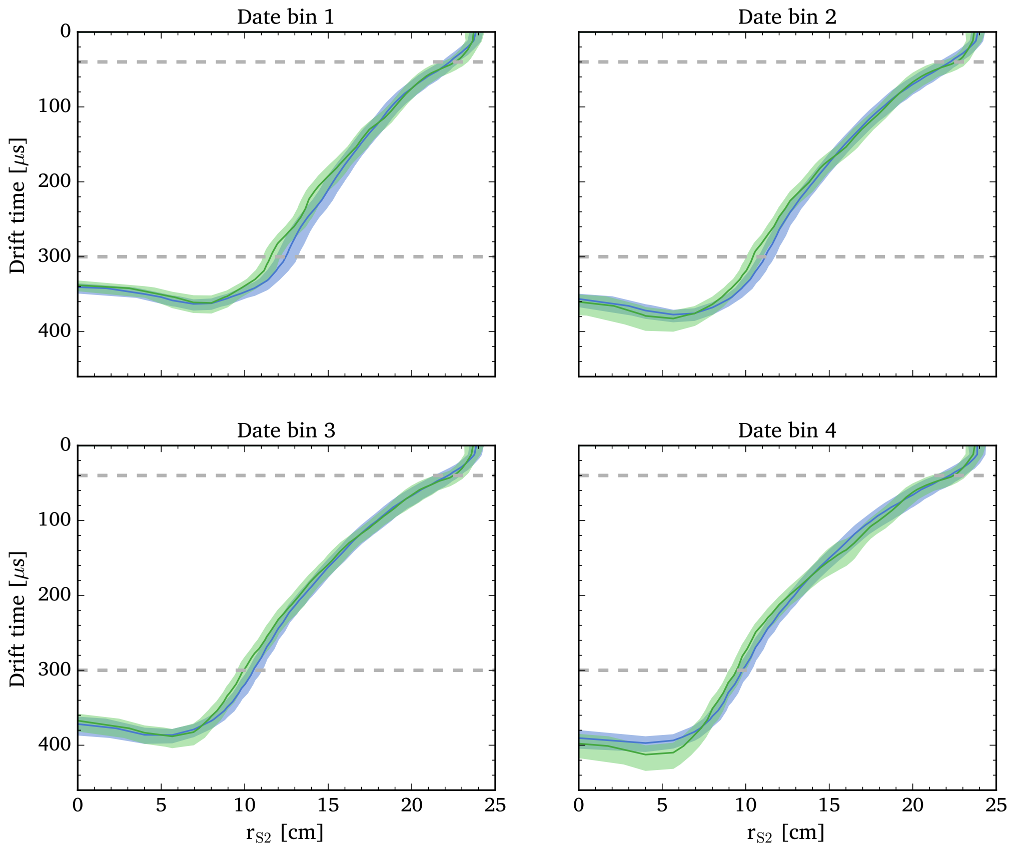

FIG. 1. A comparison of the measured position of the detector wall and cathode to that predicted by the best-fit electrostatic field model. As the electrons are drifted upwards, they are pushed radially inwards; they therefore exit the liquid surface (where they are detected and their x-y position is measured) at a radius that is less than the radius at which they originated. As a result, the measured shape of the detector wall, which is physically vertical, is warped in observed coordinates. Similarly, though the cathode is physically horizontal, the field-dependent drift velocity of electrons in liquid xenon causes its shape to appear as an inverted 'U' in measured coordinates. In each of the four axes, the blue contour is the measured shape of the detector wall from calibration data, while the green contour indicates the prediction of the wall shape from the best-fit field model. The width of each contour indicates the uncertainty in the wall position resulting from the histogram bin sizes used to construct the contours. Note that the radius of the wall in observed coordinates ("$\mathrm{r_{S2}}$") is not axially symmetric, and therefore the contours here represent an average over azimuthal angle (this is not the fit space; the fits are instead performed in 3-D). The background model for events from radon plate-out on the walls is constructed directly in measured coordinates entirely from side bands, and does not use these field maps. Horizontal gray-dashed lines, at 40 and 300 μs, indicate the drift-time extent of the fiducial volume used in WS2014–16.